Supporting Information

Anchoring Charge Selective Self-Assembled Monolayers for Tin–Lead Perovskite Solar Cells

*Zuhong Zhang, Rui Zhu, Ying Tang, Zhenhuang Su, Shuaifeng Hu, Xu Zhang, Junhan Zhang, Jinbo Zhao, Yunchang Xue, Xingyu Gao, Guixiang Li, Jorge Pascual, Antonio Abate, Meng Li.**

Z. Zhang, Dr. R. Zhu, Y. Tang, X. Zhang, J. Zhao, Y. Xue, Prof. Dr. M. Li
Key Lab for Special Functional Materials of Ministry of Education, National & Local Joint Engineering Research Center for High-efficiency Display and Lighting Technology, School of Materials Science and Engineering, and Collaborative Innovation Center of Nano Functional Materials and Applications, Henan University
Kaifeng 475004, P. R. China
E-mail: mengli@henu.edu.cn

Dr. Z. Su, J. Zhang, Prof. Dr. X. Gao
Shanghai Synchrotron Radiation Facility (SSRF)
Shanghai Advanced Research Institute
Chinese Academy of Sciences
239 Zhangheng Road, Shanghai 201204, P. R. China.

Dr. S. Hu
Clarendon Laboratory
Department of Physics
University of Oxford
Parks Road, Oxford, OX1 3PU

Dr, J. Pascual
POLYMAT, University of the Basque Country UPV/EHU
Centro Joxe Mari Korta Center
Tolosa Avenue, 72, 20018 Donostia-San Sebastián, Spain

Dr. G. Li
Institute of Chemical Sciences and Engineering
École Polytechnique Fédérale de Lausanne (EPFL)
CH-1015 Lausanne, Switzerl

Dr. G. Li, Prof. Dr. A. Abate
Helmholtz-Zentrum Berlin für Materialien und Energie GmbH
Hahn-Meitner-Platz 1, 14109 Berlin, Germany.

Experimental

Materials

Lead iodide (99.999%), tin iodide (SnI_2, 99.999%), tin fluoride (SnF_2, 99.999%), fullerene (C_{60}, 99.9%), bathocuproine (BCP, 99.9%), ammonium thiocyanate (NH_4SCN, 99.99%), glycine hydrochloride (GlyHCl, 99%) and F-doped tin oxide (FTO) were purchased from Libra Technology Corporation. Formamidinium iodide (FAI, 99.99%) and methylammonium iodide (MAI, 99.99%) were purchased from GreatCell Solar (Australia). Cesium iodide (CsI, 99.999%) was purchased from Xi'an Yuri Solar Co., Ltd. (9-carbazolyl)acetic acid (9CAA, 95%) and 3-(9-Carbazolyl)propionic acid (9CPA, 95%) was purchased from Macklin. 2-(9H-Carbazol-9-yl)ethyl]phosphonic acid (2PACz, 98%) was purchased from TCI. Chlorobenzene (CB, 99.8%, SuperDry, with molecular sieves), *N*,*N*-dimethylformamide (DMF, 99.8%, SuperDry, with molecular sieves), dimethyl sulfoxide (DMSO, 99.7%, SuperDry, with molecular sieves), ethanol and isopropanol (IPA, 99.5%, SuperDry, with molecular sieves) were purchased from J&K scientific.

Fabrication of tin-lead PSCs

Previous preparation: 46.8 mg CsI, 185.7 mg FAI, 85.8 mg MAI, 14.1 mg SnF_2, 414.9 mg PbI_2, 335.3 mg SnI_2, 2.7 mg NH_4SCN and 4.0 mg GlyHCl were dissolved in 1 mL mixed solvents of DMF: DMSO (3:1) to stir for 10 hours at 60 ℃. 2PACz, 9CPA and 9CAA were dissolved in ethyl alcohol (0.3 mg/mL). FTO was ultrasonically cleaned in turn by deionized water, acetone, and ethyl alcohol for 15 minutes.

Devices preparation: The cleaned FTO were cleaned O_3 for 30 minutes. After that, FTO was shifted to an N_2-filled glovebox by transfer bunker. 100 μL SAM solutions were spin-coated on FTO (600 rpm/s, 3000 rpm, 30 seconds). After the end, FTO/SAMs were annealed for 10 minutes on a 100 ℃ heating table. After annealing, 100 μL perovskite precursor solution was spin-coated on FTO/SAMs (600 rpm/s, 1000 rpm, 10 seconds and 2000 rpm/s, 4000 rpm, 40 seconds) and the drip time of the antisolvent is 20 seconds of the second step. After the end, the FTO/SAMs/perovskites were annealed for 10 minutes on a 100 ℃ heating table. After annealing, the FTO/SAMs/perovskites were shifted to a vacuum evaporation apparatus. Before evaporation, the vacuum degree stayed below 10^{-4} Pa. After that, 15 nm BCP (0.02-0.03 nm/s), 35 nm C_{60} (0.03-0.05 nm/s) and 110 nm Ag electrode were evaporated in turn using 0.13 cm^2 mask.

Characterization

Crystallinity was performed via grazing-incidence wide-angle X-ray scattering (GIWAXS, BL14B1 beamline of the Shanghai Synchrotron Radiation Facility (SSRF) using X-ray with a wavelength of 0.6887 Å) and X-ray diffractometer (XRD, Rigaku D/MAX-2400 diffractometer). Surface morphology was performed by top view scanning electron microscope (SEM, Zeiss, Supra55, SE2 pattern under 5 KV). Energy band alignment was obtained from ultraviolet photoelectron spectroscopy (UPS, Specs, PHOIBOS 100, Helium lamp) measurement. Contact potential difference (CPD) was performed by atomic force microscope (AFM, SPA400, Zeiss). Series and recombination resistance were obtained from Electrochemical impedance spectroscopy under dark conditions. (EIS, Electrochemical Workstation, Netherlands). Transient photocurrent (TPC) and transient photovoltage (TPV) were performed by transient photocurrent/voltage tester (Shanghai Jinzhu Technology Co., LTD, laser 570 nm). V_{OC} versus light intensity changing, dark current-voltage (*J*–*V*), space-charge-limited current (SCLC), conductivity and current-voltage (*J*–*V*, 10 mV/s, 100 mW/cm^2, standard silicon solar cell calibration) were performed sunlight simulator with a digital source meter. (IVX-50, EnLi Technology, Taiwan). Mott−Schottky measurement was performed by Electrochemical impedance spectroscopy under dark conditions. (EIS, Electrochemical Workstation, Netherlands). Trap density of states (t-DOS) was performed via a Precision impedance analyzer (Agilent 4294A).

Transmittance and absorption were performed by Ultraviolet-visible (UV-vis) absorb spectrum (PE Lambda 950).

Computational formula

V_{OC} versus changing light intensity: $V_{OC} = n\frac{K_B T}{q} lnI$, where n, K_B, T, q and I are the ideal factor, the Boltzmann constant, the temperature, the elementary charge and the normalized light intensity, respectively[1].

Space-charge-limited current (SCLC): $N_t = \frac{2\varepsilon\varepsilon_0 V_{TEL}}{qL^2}$, where N_t, ε, ε_0, V_{TEL}, q and L are the trap density, the relative dielectric constant of perovskite, the vacuum dielectric constant, the trap-filled limit voltage, the elementary charge and perovskite film thickness, respectively[2].

Trap density of states (t-DOS): $tDOS\ (E_\omega) = \frac{V_{bi}\omega dC}{qWK_B T d\omega}$, where V_{bi}, ω, C, q, W, K_B and T are the built-in potential, the angular frequency, the capacitance, the elementary charge, the depletion width, Boltzmann constant and the temperature, respectively[3].

Conductivity: $\sigma = \frac{AV}{dJ}$, where A, V, d and J are the active area, the voltage, the thickness and current, respectively[4].

Calculation

For revealing the interface structure and transfer property, the SAMs/perovskite interface model was constructed and simulated by the first principles methods. What should be noted is that the Cs^+ was used to replace FA^+, because it is not involved in VBM and CBM, and the interaction between SAMs with FA^+ can be ignored.

First, to construct the $CsSn_{0.5}Pb_{0.5}I_3$ perovskite mode, the cubic phase $CsPbI_3$ and $FASnI_3$ crystal structure were chosen and optimized at a plane-wave pseudopotential approach with Perdew−Burke−Ernzerhof (PBE) functional as implemented in the Vienna Ab initio Simulation Package (VASP) code. In particular, the convergence criteria for atomic forces were set at less than 0.01 eV/Å, and total energies were converged to 10−5 eV. A cutoff energy of 450 eV was used for the plane-wave basis set in all calculations. For Brillouin zone integration, we employed a k-point grid of 3 × 3 × 3 for bulk. As shown in Table S1, the calculations are very accurate, with a margin of error of 0.39% and 0.60% for $CsPbI_3$ and $CsSnI_3$, respectively. Then, based on the two structures, $CsPb_{0.5}Sn_{0.5}I_3$ structures were constructed, through three crystal axis directions building a supercell containing 2 cells, and one Sn replaced the Pb atom in the supercell. After optimizing the six structures using the VASP package, it was found that there was no significant difference in these structures. Therefore, the $CsPb_{0.5}Sn_{0.5}I_3$ structure constructed in a direction was chosen for calculation. Later, a (001) $CsPb_{0.5}Sn_{0.5}I_3$ surface with CsI- termination was used as the interface. For describing the real interface process a 3 × 2 × 3 supercell was used and a 15 Å vacuum layer to separate adjacent surfaces in the c-axis direction and construct.

Secondly, the SAMs molecular structures of 2PACz, 9CPA, and 9CAA were firstly optimized with the B3LYP functional and the basis set was 6-31+(d, p) within the Gaussian 16 package. Then, the CCSD functional and 6-311+(d, p) basis set were used to estimate the single point energy, nature bond orbital and electrostatic potential of singlet SAM molecules.

Finally, three types of SAMs/$CsPb_{0.5}Sn_{0.5}I_3$ structures were constructed by building molecules on the surface of perovskite. Structure optimizes and Partial Density of State (PDOS) and charge transfer property was simulated in CP2K package, where PBE-D3 functional was used with double-zeta basis sets (DZVP-MOLOPT) and Goedecker–Teter–Hutter pseudopotentials.

Table S1 Calculating parameters.

Component	Lattice constant	Experimental (Å)	Optimized (Å)	Error (%)
$CsPbI_3$	a	6.2965	6.2720	0.39
$CsSnI_3$	a	6.2057	6.1687	0.60
	a	12.5439	12.5127	
$CsPb_{0.5}Sn_{0.5}I_3$	b	6.2720	6.2593	
	c	6.2720	6.2593	

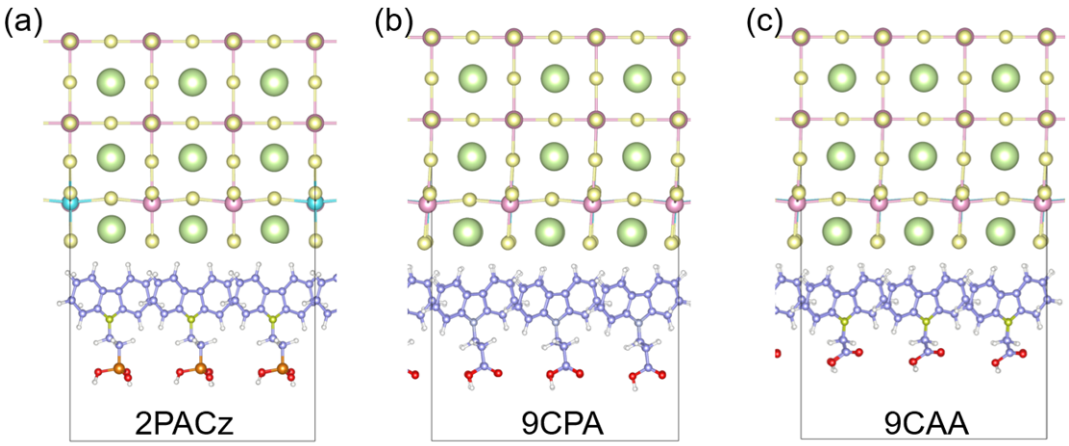

Figure S1. The top views of a) 2PACz/perovskite, b) 9CPA/perovskite and c) 9CAA/perovskite structures.

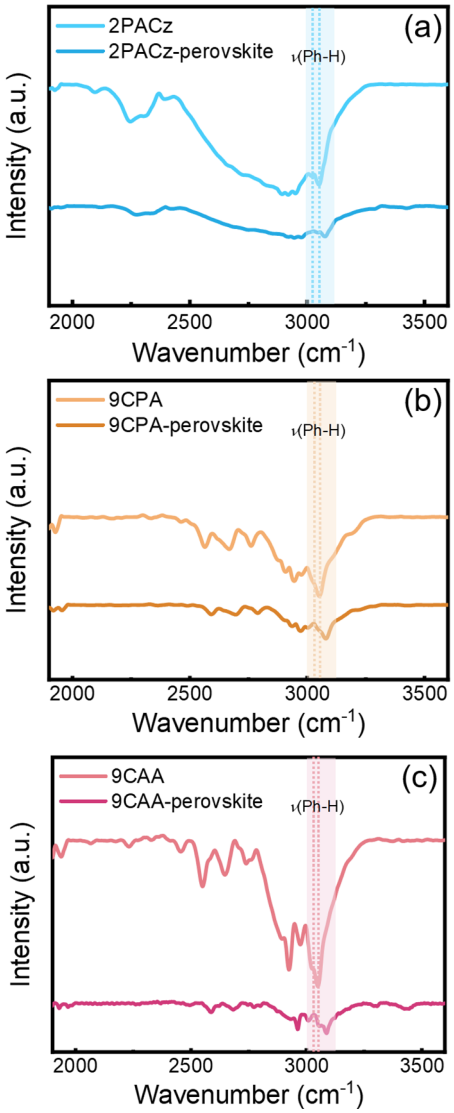

Figure S2. FTIR spectrum of a) 2PACz and when combined with perovskite, b) 9CPA and when combined with perovskite, c) 9CAA and when combined with perovskite.

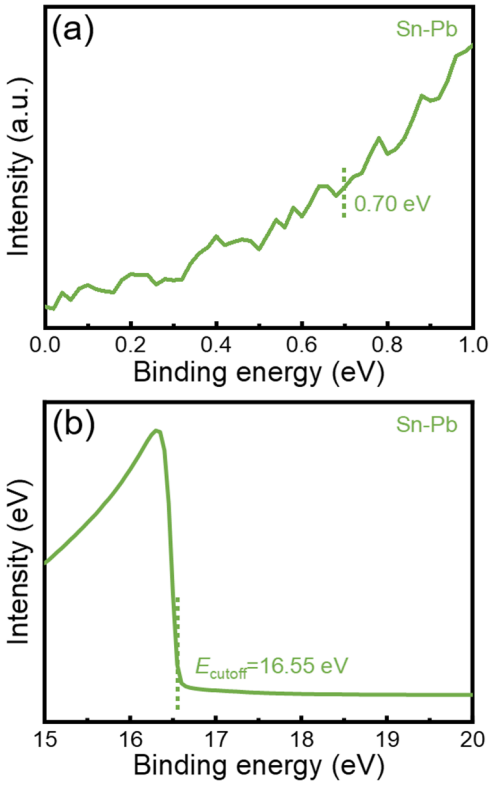

Figure S3. a) E_i plot and b) E_{cutoff} plot of Sn–Pb perovskite from UPS measurement.

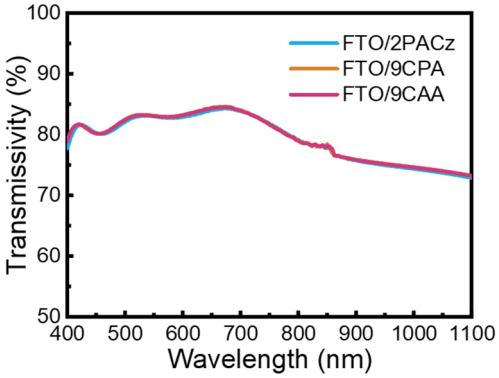

Figure S4. Transmissivity curves of FTO/SAMs.

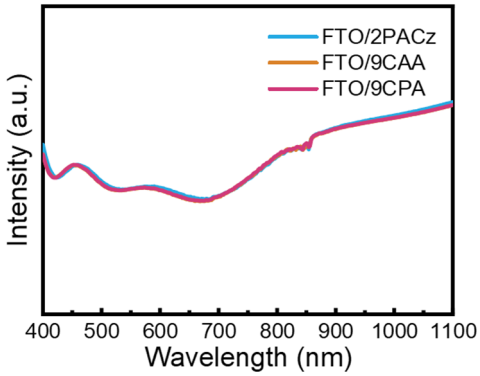

Figure S5. UV-vis absorb spectrum curves of FTO/SAMs.

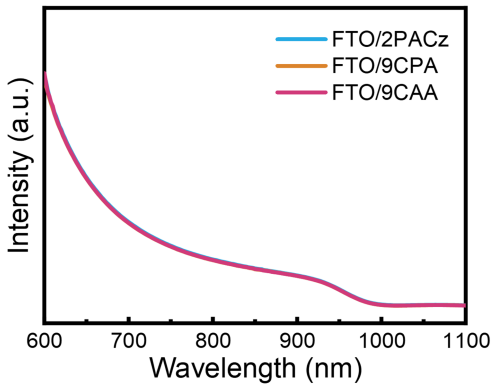

Figure S6. UV-vis absorb spectrum curves of FTO/SAMs/perovskite.

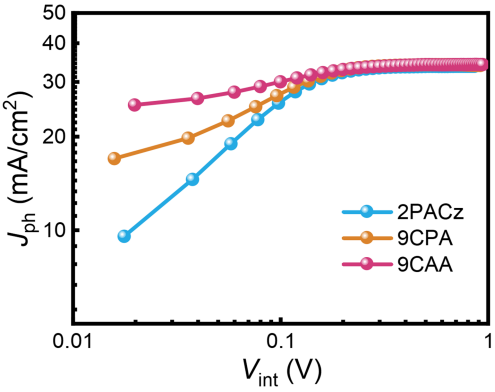

Figure S7. J_{ph} versus V_{int} curves of full devices.

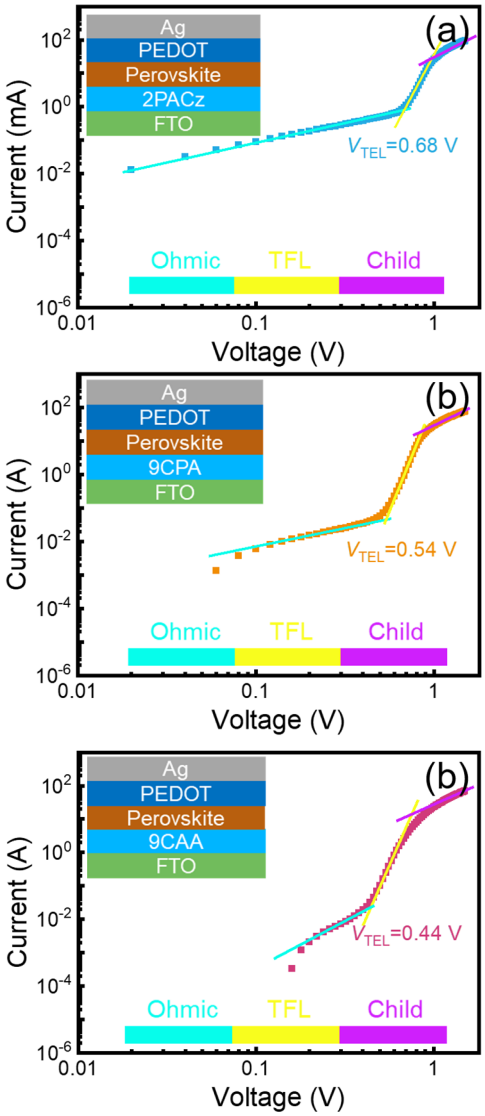

Figure S8. SCLC based on the structure of a) FTO/2PACz, b) /9CPA, c) and /9CAA/perovskite/PEDOT/Ag.

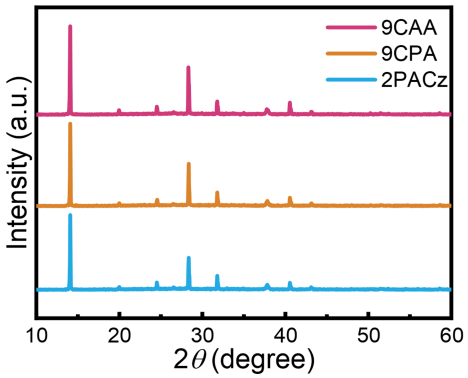

Figure S9. XRD plots of perovskite based on FTO/SAMs.

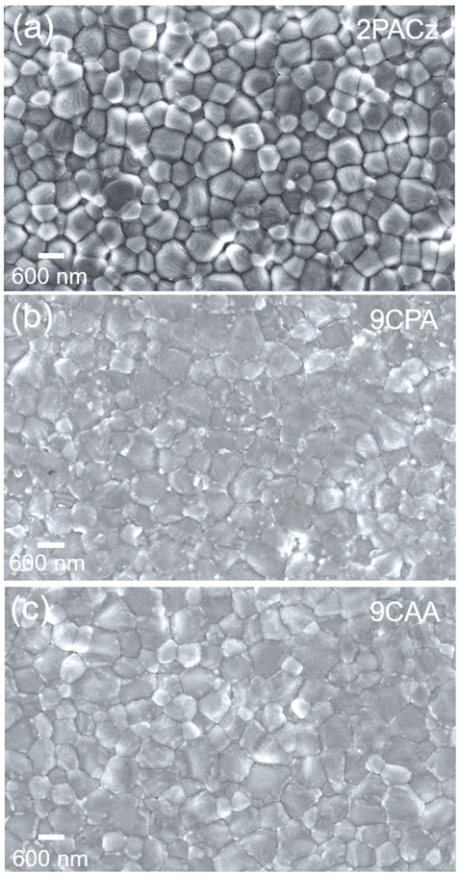

Figure S10. Top view SEM images of perovskites based on a) FTO/2PACz, b) 9CPA and c) 9CAA.

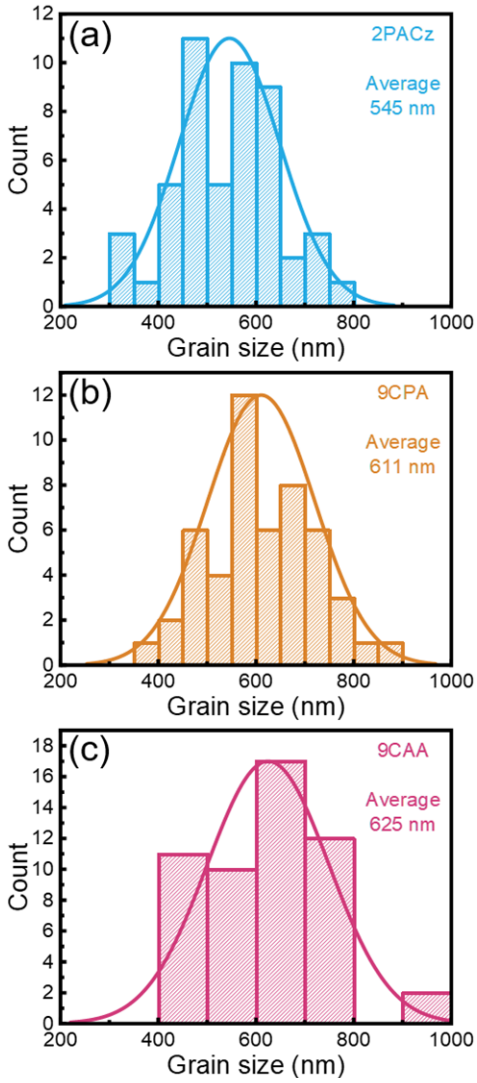

Figure S11. Grain size histogram of perovskites based on FTO/a) 2PACz, b) 9CPA and c) 9CAA.

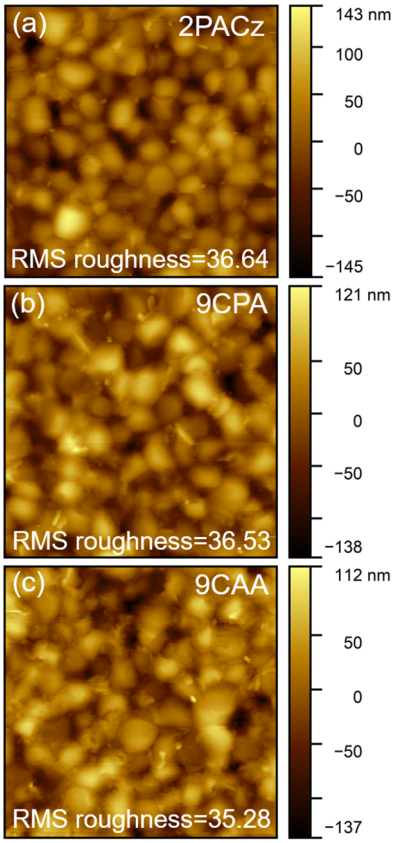

Figure S12. AFM images of perovskites based on a) 2PACz, b) 9CPA and c) 9CAA.

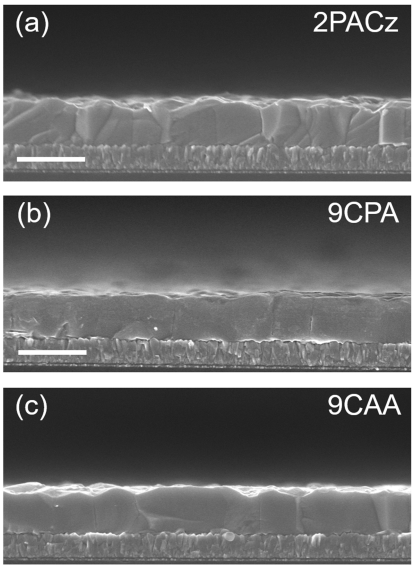

Figure S13. SEM cross section of perovskite films based on a) FTO/2PACz, b) FTO/9CPA and c) FTO/9CAA. The scale bar is 1 μm

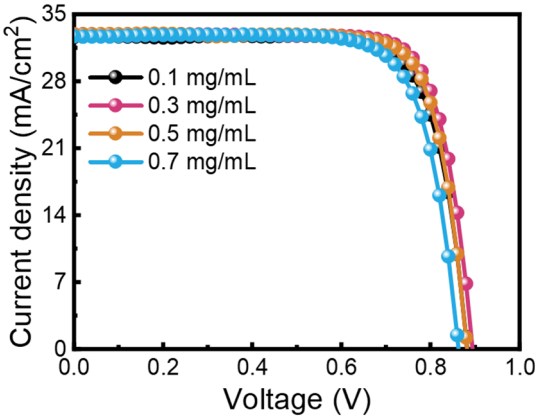

Figure S14. J-V curves of devices based on 0.1, 0.3, 0.5 and 0.7 mg/mL.

Table S2 Summarized PV parameters of PSCs based on 0.1, 0.3, 0.5 and 0.7 mg/mL 9CAA, respectively.

Concentration (mg/mL)	***V*OC (V)**	***J*SC (mA/cm^2)**	**FF (%)**	**PCE (%)**
0.1	0.89	32.6	76	22.1
0.3	0.9	32.9	78	23.1
0.5	0.89	32.9	78	22.9
0.7	0.87	32.7	76	21.7

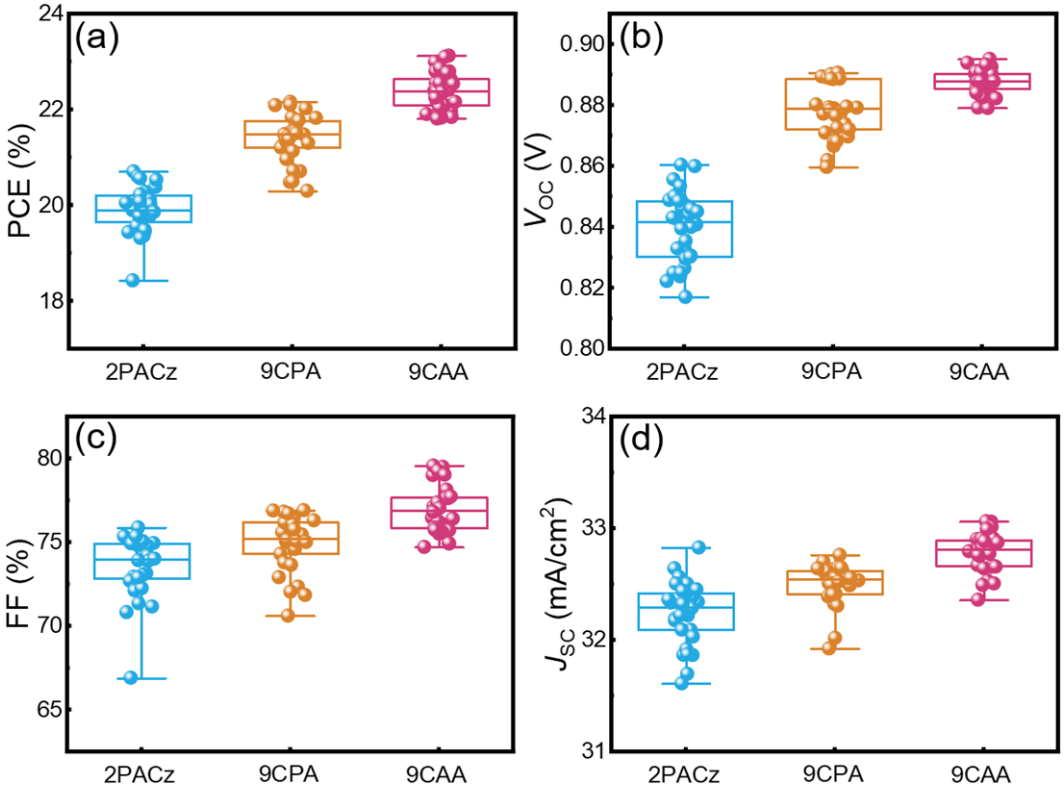

Figure S15. Box-type statistical diagram of a) PCE, b) V_{OC}, c) FF and d) J_{SC} based on more than 20 devices.

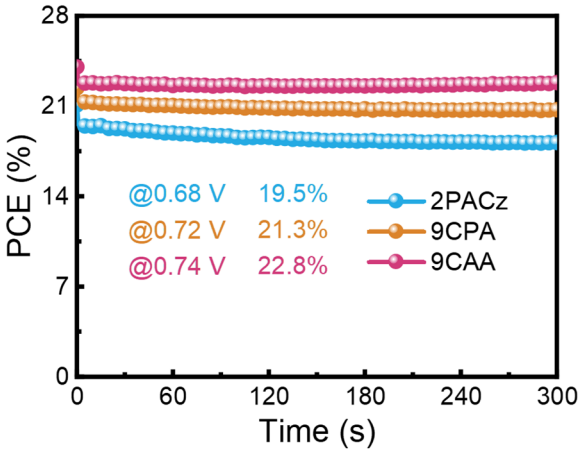

Figure S16. MPP tracking curves of full devices.

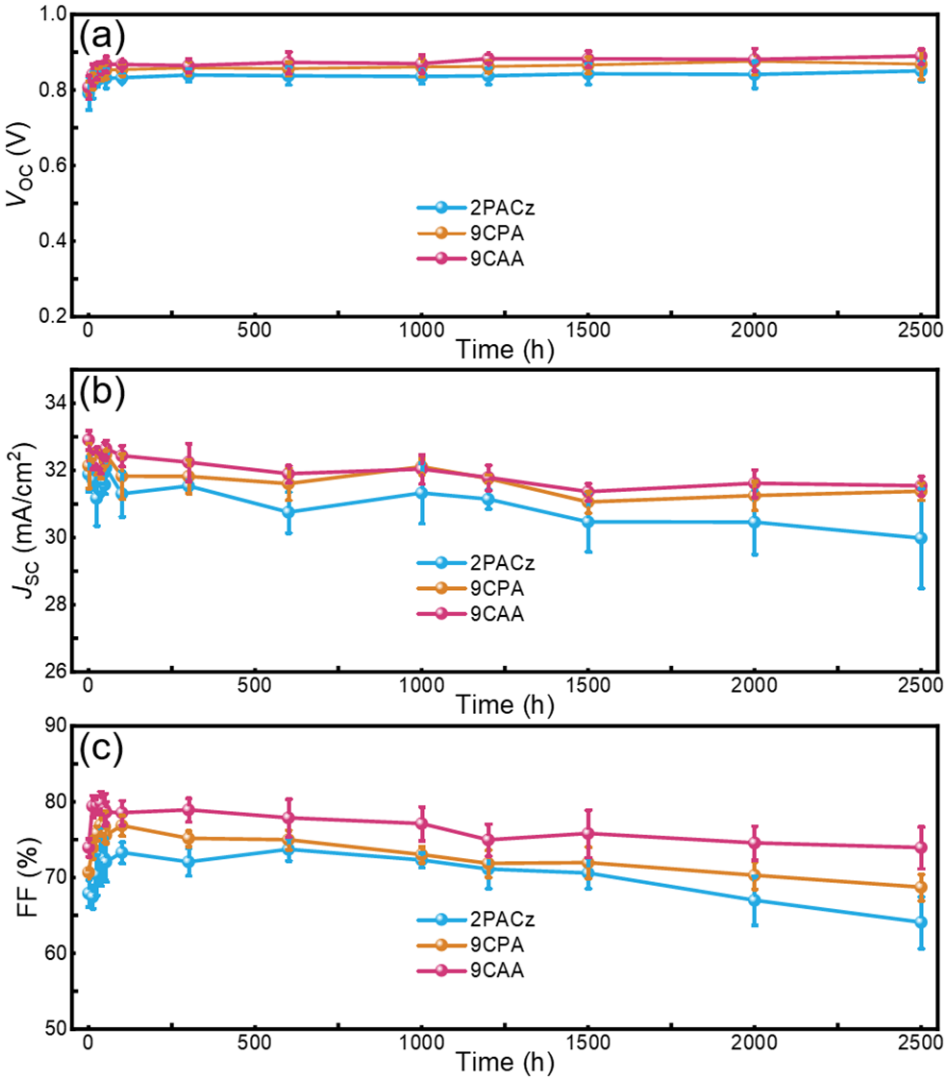

Figure S17. Stability curves of a) V_{OC}, b) J_{SC} and c) FF parameters, based on full devices in N_2 atmosphere.

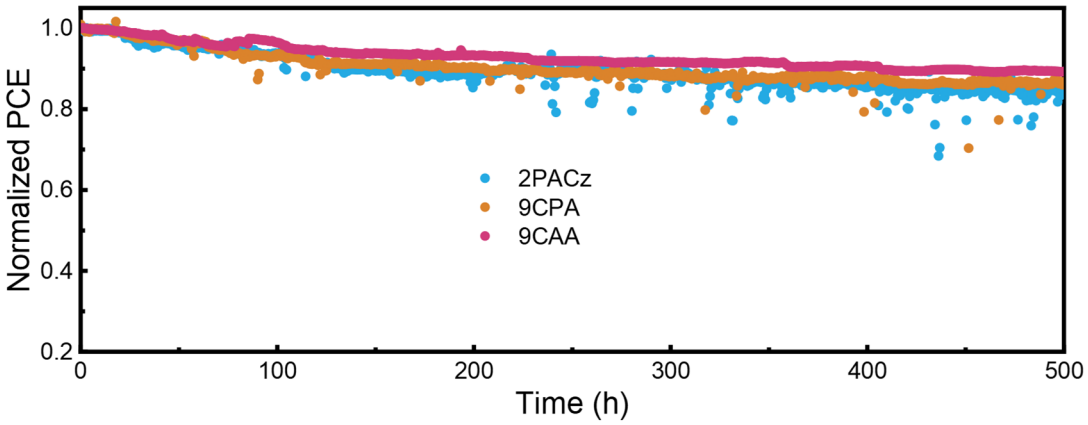

Figure S18. Continuous MPP tracking for encapsulated PSCs under AM 1.5 illumination (white LED) in ambient air.

Reference

[1] J. Zhang, Y. Sun, C. Huang, B. Yu, H. Yu, *Adv. Energy Mater.* **2022**, *12*, 2202542.

[2] R. Wang, A. Altujjar, N. Zibouche, X. Wang, B. F. Spencer, Z. Jia, A. G. Thomas, M. Z. Mokhtar, R. Cai, S. J. Haigh, J. M. Saunders, M. S. Islam, B. R. Saunders, *Energy Environ. Sci.* **2023**, *16*, 2646.

[3] T. Wang, Y. Li, Q. Cao, J. Yang, B. Yang, X. Pu, Y. Zhang, J. Zhao, Y. Zhang, H. Chen, A. Hagfeldt, X. Li, *Energy Environ. Sci.* **2022**, *15*, 4414.

[4] C. Xu, S. Zhang, W. Fan, F. Cheng, H. Sun, Z. Kang, Y. Zhang, *Adv. Mater.* **2023**, *35*, 2207172.